PACS numbers: 42.79.Qx; 85.60.Gz
DOI: 10.1070/QE2004v034n12ABEH002648

Effect of the quantum nature of detecting low-intensity radiation on the distance measurement error in pulsed laser ranging

E.V. Buryi, Yu.L. Smirnova

***Abstract*. The dispersion of estimates of the time position of low-intensity radiation pulses is studied as a function of their duration and detection parameters. Simulations showed that the error of distance measuring to an object in one ranging cycle can be 0.05 – 0.10 m. The method for obtaining precision estimates of a distance to objects without corner reflectors is proposed.**

Keywords: *laser pulse, laser ranging, distance measurement error.*

1. Introduction

A promising direction in the development of the methods for signal processing in pulse laser ranging used for precision measuring distances to remote objects (for example, Earth satellites) is the analysis of counts of signal realisations at the photodetector (PD) output formed by a fast analog-to-digital converter (ADC). The algorithms for realisation processing should be developed taking into account the statistical characteristics of signals and noise as well as the PD and ADC parameters.

When the intensity of detected radiation is low, the statistical parameters of the noise substantially differ from those for the Gaussian process, and therefore the known estimates of the efficiency of processing methods, which are widely used in radiolocation, cannot be employed in the synthesis of systems for processing such laser ranging signals. In this case, the potential possibilities of various methods for signal processing can be analysed and the requirements to the technical means for detecting and transformation of signals can be determined most efficiently by using simulations of signal realisations at the PD output, which takes into account the quantum nature of radiation detection.

2. Physical model of the photodetection process

It is known [1, 2] that photodetection is a quantum-mechanical process because a flow of primary photoelectrons is formed in a PD illuminated by radiation of a constant intensity, the probability $P(n, t)$ of appearance of n photoelectrons detected in the observation interval $[t_0, t_0 + T]$ being described by the Poisson law

$$P(n, T) = \frac{\langle n \rangle^n}{n!} \exp(-\langle n \rangle), \quad (1)$$

where $\langle n \rangle = \eta W/(h\nu)$ is the mean number of photoelectrons in this interval; η is the quantum efficiency of the PD; $h\nu$ is the photon energy;

$$W = \int_{t_0}^{t_0+T} \left[\int_{S_{\rm d}} I(\boldsymbol{r}, t) \mathrm{d}\boldsymbol{r} \right] \mathrm{d}t$$

is the energy of detected radiation; and $I(\boldsymbol{r}, t)$ is the radiation intensity at different points on the PD surface $S_{\rm d}$ determined by the radius vector $\boldsymbol{r}$. Because $I(\boldsymbol{r}, t)$ is a random function of time, expression (1) should be interpreted as the conditional probability p that the random quantity W takes the value w:

$$p(n|W = w, T) = \frac{1}{n!} \left(\frac{\eta w}{h\nu} \right)^n \exp\left(-\frac{\eta w}{h\nu} \right). \quad (2)$$

By using a semiclassical method for establishing the relation between the statistic properties of optical fields and corresponding photoelectron counts proposed by Mandel [3] and by averaging $p(n|W = w, T)$ over the probability density of the optical signal energy distribution $p_W(w)$, we obtain

$$P(n, T) = \int_0^\infty p(n|W = w, T) p_W(w) \mathrm{d}w$$

$$= \int_0^\infty \frac{1}{n!} \left(\frac{\eta w}{h\nu} \right)^n \exp\left(-\frac{\eta w}{h\nu} \right) p_W(w) \mathrm{d}w,$$

from which it follows that the distribution $P(n, T)$ substantially differs in the general case from the Poisson distribution.

The time dependence of the PD output current $i(t)$ is determined by the parameters of a flow of primary photoelectrons. For high energies W of the detected radiation, the dependence $i(t)$ is a continuous function of time, whereas for low W and the equivalent pass band of the PD exceeding $1/T$, the so-called one-electron current pulses are detected at the PD output.

Because the thermal noise of semiconductor PDs is large, we will consider the output signal of a vacuum PD – a

E.V. Buryi, Yu.L. Smirnova Scientific-Research Institute of Radioelectronics and Laser Technology, N.E. Bauman Moscow State Technical University, ul. 2-ya Baumanskaya 5, 1007005 Moscow, Russia; web-site: www.llis.bmstu.ru; e-mail: buryi@bmstu.ru

Received 15 March 2004; revision received 7 September 2004
Kvantovaya Elektronika **34** (12) 1147 – 1150 (2004)
Translated by M.N. Sapozhnikov

photomultiplier. The theory of photoemission [4] is based on the assumption that the probability of escape of a primary photoelectron from a photocathode in a small time interval Δt is proportional to the instant intensity of optical radiation. Such events in different time intervals are statistically independent and the probability of emission of more than one photoelectron $P(n, \Delta t)$ (where $n = 2, 3, ...$) is a quantity of a greater smallness order than $P(1, \Delta t)$. In the general case, we can assume that the dependence $i(t)$ at the photomultiplier output is a superposition of one-electron pulses

$$i(t) = \int_{-\infty}^{\infty} \chi\xi(\tau)h(t - t_{\rm d} - \tau)d\tau, \tag{3}$$

where χ is the one-electron pulse amplitude, which is a random quantity because of fluctuations of the multiplication factor of the photomultiplier; $\xi(t) = \sum_n \delta(t - \tau_n)$ is the realisation of a random flux of primary photoelectrons formed at instants τ_n; $h(t - t_{\rm d})$ is the function of the pulse response of the dynode system and the output circuit of the photomultiplier to the unit event of the primary photoelectron formation; $t_{\rm d}$ is the time interval between the instant t of the primary electron formation and the instant of the maximum of the one-electron pulse. The amplitude of the one-electron pulse is characterised by the distribution density $p_\chi(A)$ [5] (Fig. 1). Note that $t_{\rm d}$ is a random quantity in the general case [4]. The dispersion of $t_{\rm d}$ substantially depends on the design of the dynode system of the photomultiplier. The dispersion of $t_{\rm d}$ for modern fast photomultipliers (for example, Hamamatsu R7400U) is much smaller than the one-electron pulse FWHM $h(t- t_{\rm d})$. Therefore, we will assume that $t_{\rm d}$ is a determinate quantity.

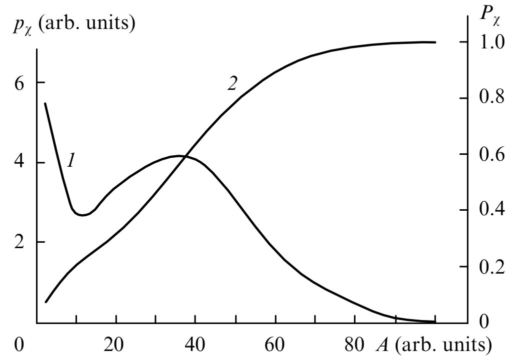

Figure 1. Amplitude distribution density $p_\chi(A)$ for the one-electron pulse (*1*) and the corresponding distribution function $P_\chi(A)$ (*2*).

3. Simulation of the PD output signal

If the average number μ of events of formation of primary photoelectrons in an observation interval $[t_0, t_1]$ is constant, we can assume that the formation of photoelectrons is described by the Poisson process. The time interval between two successive events in such a process occurring at times τ_{n-1} and τ_n, where $t_0 < \tau_{n-1} < \tau_n < t_1$, has an exponential distribution with the parameter μ [6]

$$P\{\tau_n - \tau_{n-1} > t|\tau_1, ..., \tau_{n-1}\}$$
$$= P\{\tau_n - \tau_{n-1} > t\} = \exp(-\mu t). \tag{4}$$

The time intervals $\tau_1 - t_0,\ \tau_2 - \tau_1, ...,\ \tau_n - \tau_{n-1}$ between these successive events are independent random quantities. If the detected radiation intensity varies within the time interval $[t_0, t_0 + T]$, condition (4) is not fulfilled. In this case, the partition

$$\Pi(t_0, t_0 + T) = \{t_l\}_{l=0}^{l=L},\quad t = t_0 < t_1 < ...t_{L-1} < t_L = t_0 + T,$$

$$t_i - t_{i-1} < \Delta t,\quad i = 1, 2, ..., L$$

of the interval $[t_0, t_0 + T]$ should be introduced so that $\Delta t \to 0$ for $L \to \infty$. Then, the energy w_i of detected radiation in each of the intervals $[t_{i-1}, t_i]$ $(i = 1, 2, ..., L)$ can be considered constant:

$$w_i = \int_{t_{i-1}}^{t_i} \left[\int_{S_{\rm d}} I(\boldsymbol{r}, t)d\boldsymbol{r}\right]dt,\quad i = 1, 2, ..., L.$$

Therefore, the detection probability distribution $p_i(n|W = w_i)$ for n photoelectrons in the interval $[t_{i-1}, t_i]$ will be described by expression (2). This means that, to simulate $\xi(t)$ upon detection of radiation with the time-dependent intensity, the observation interval T should be divided into L subintervals, and a Poisson flux of events in each of them should be simulated using the distribution function corresponding to the radiation energy in this subinterval. Taking into account the additivity of the exponential distribution, the sequence of time intervals $\{\tau_i^j\}_{j=1}^N$ should be simulated in the ith interval under study as long as the inequality

$$\tau_i^{N_i} = \tau_i^{N_i-1} + \tau \leqslant t_i$$

is valid, where N_i the number of the last simulated event in this interval and τ is the realisation of the random quantity having exponential distribution law (4) with the parameter

$$\mu_i = \frac{1}{t_i - t_{i-1}}\frac{\eta w_i}{hv},$$

which is obtained from the realisation $\tau = -\ln(1 - z)/\mu_i$ of a random quantity z uniformly distributed in the $[0, 1]$ interval [6].

By combining the sequences $\{\tau_i^j\}_{j=1}^N$ found for all the intervals $[t_{i-1}, t_i]$ $(i = 1, 2, ..., L)$ into one sequence $\{\tau_n\}_{n=1}^N = \{\tau_1^1, ..., \tau_1^{N_1}, \tau_2^1, ..., \tau_2^{N_2}, ..., \tau_L^1, ..., \tau_L^{N_L}\}$, where $N = \sum_{i=1}^L N_i$ is the total number of events in the interval $[t_0, t_0 + T]$, we obtain the required realisation

$$\xi(t) = \sum_{n=1}^N \delta(t - \tau_n).$$

Having found N realisations $\chi_1, ..., \chi_N$ of the random quantity χ from the equation $\chi_n = P_\chi^{-1}(z_n)$ (where $P_\chi(A)$ is the distribution function of the random quantity χ and z_n are the realisations of the random quantity uniformly distributed in the interval $[0, 1]$) and using (3), we obtain the realisation

$$i(t) = \sum_{n=1}^N \chi_n h(t - t_{\rm d} - \tau_n)$$

of the output current of the photomultiplier.

4. Dependence of the distance measurement error on the conditions of object location and methods of signal processing

Because the average intensity of the photoelectron flux produced by background radiation during the Earth satellite ranging is, as a rule, within $(4-5)\times10^5$ s^{-1}, while the main parameters of the satellite orbit are known, we can assume that the reflected signal can be reliably detected in the observation interval 50 – 100 ns for $\langle n\rangle = 1-10$ [7]. Because the probability of detection of noise photoelectrons in this interval does not exceed 5×10^{-2}, their influence on the results of measurements can be neglected.

The time interval between the instant t_f of the laser pulse radiation and the instant t_r of the reflected signal detection is estimated, as a rule, by threshold methods [8, 9]. The main disadvantage of the threshold methods is the dependence of the measurement error of t_r on the shape and amplitude of the output pulse of the photomultiplier. As a rule, this error exceeds the error of measuring the time interval caused by fluctuations of the refractive index of the atmosphere [7]. The digitisation of the signal $i(t)$ with the period T_d and N_q quantisation levels allows one to obtain the estimates of t_r from the positions of the maximum of the likelihood function [9], the centre of gravity t_r^g of the pulse, and the event t_r^th of the adapted threshold crossing on the time axis or to estimate the model time t_r^m at which the model envelope $i^\mathrm{m}(t)$ of the pulse corresponds best of all to the realisation $i(t)$ within the interval $[t_0, t_0+T]$. Because the determination of multidimensional conditional probability densities of observed realisations $i(t)$ is extremely time consuming, while the use of optimisation methods for determining t_r^m cannot guarantee in the general case the solution stability, we analysed the estimates of t_r^g and the estimates of $t_\mathrm{r}^\mathrm{th1}$ and $t_\mathrm{r}^\mathrm{th2}$ obtained by two methods:

$$t_\mathrm{r}^\mathrm{th1} = t_0 + T_\mathrm{d}\{k + [i_\mathrm{th} - i(t_k)]/[i(t_{k+1}) - i(t_k)]\},$$

$$i(t_k) \leqslant i_\mathrm{th} < i(t_{k+1}),$$

$$t_\mathrm{r}^\mathrm{th2} = t_0 + 0.5T_\mathrm{d}\{k + [i_\mathrm{th} - i(t_k)]/[i(t_{k+1}) - i(t_k)]$$

$$+ l + [i(t_l) - i_\mathrm{th}]/[i(t_l) - i(t_{l+1})]\},\ i(t_k) \leqslant i_\mathrm{th} < i(t_{k+1}),$$

$$i(t_l) > i_\mathrm{th} \geqslant i(t_{l+1}),$$

where $i_\mathrm{th} = 0.5\max[i(t_1), i(t_2), ...]$ is the threshold calculated for each of the realisations of $i(t)$; and k and l are the numbers of time intervals within which the first and last threshold crossings i_th are observed.

The errors of measuring t_r by different methods were estimated by using statistical simulation of the procedures of formation of the estimates t_r^g, $t_\mathrm{r}^\mathrm{th1}$, and $t_\mathrm{r}^\mathrm{th2}$ of the realisations $i(t)$ corresponding to the Gaussian shape of probe pulses with different FWHMs $\tau_{0.5}$ (Fig. 2). To determine the potentially achievable measurement accuracy, we also analysed the estimates of $\tilde{t}_\mathrm{r}^\mathrm{g}$, $\tilde{t}_\mathrm{r}^\mathrm{th1}$, and $\tilde{t}_\mathrm{r}^\mathrm{th2}$ obtained for rectangular pulses. The realisations of $i(t)$ were simulated under the condition that the energies of detected pulses of different duration and shape were the same. Figure 3 shows the calculated dispersions $\sigma^2(\langle n\rangle)$ of the required estimates. Also, the dependence of the number of failures (gross

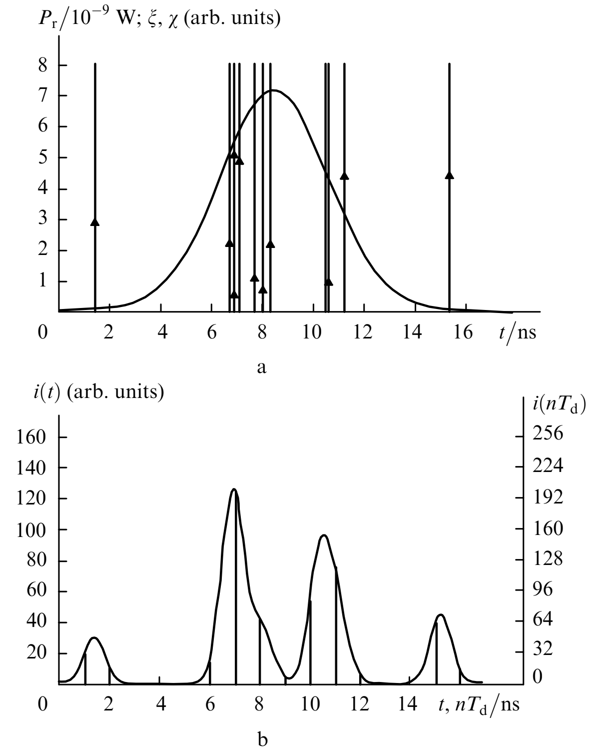

Figure 2. Simulations of the flux of primary photoelectrons (a) and the output signal of a photomultiplier (b): detected radiation pulse $P_\mathrm{r}(t)$ of duration 5 ns for $\langle n\rangle = 10$ (solid curve), realisation $\xi(t)$ (vertical straight lines) and the corresponding values of χ (▲); realisation $i(t)$ (solid curve) and counts $i(nT_\mathrm{d})$ at the ADC output for $N_\mathrm{q} = 256$ and $T_\mathrm{d} = 1$ ns (vertical straight lines).

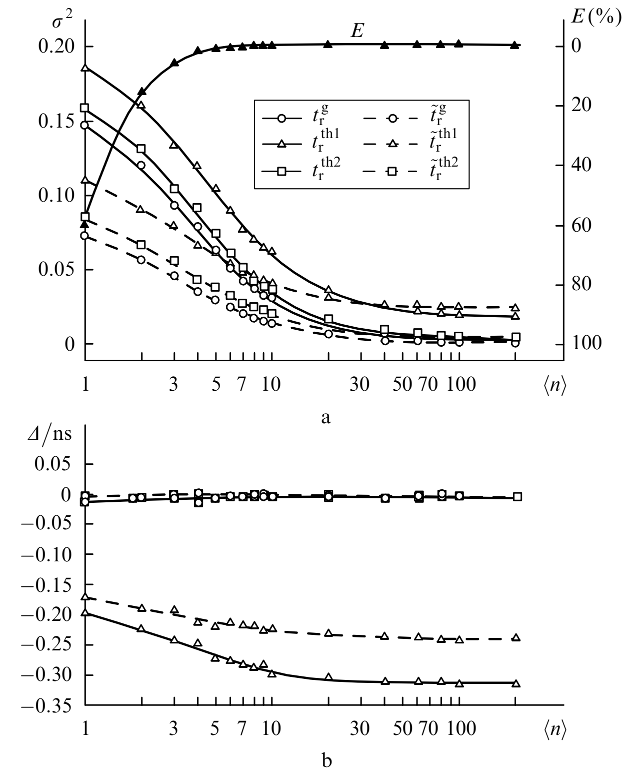

Figure 3. Characteristics of the estimates t_r^g, $\tilde{t}_\mathrm{r}^\mathrm{g}$, $t_\mathrm{r}^\mathrm{th1}$, $\tilde{t}_\mathrm{r}^\mathrm{th1}$, $t_\mathrm{r}^\mathrm{th2}$, and $\tilde{t}_\mathrm{r}^\mathrm{th2}$ of the time position of the detected Gaussian (solid curves) and rectangular (dashed curves) pulses for $\tau_{0.5} = 1$ ns, $T_\mathrm{d} = 1$ ns, and $N_\mathrm{q} = 256$: the dispersions $\sigma^2(\langle n\rangle)$ of estimates and the number $E(\langle n\rangle)$ of failures (a) and deviations $\Delta(\langle n\rangle)$ of these estimates from their real values (b).

measurement errors appearing due to the absence of signal one-electron pulses in the observation interval) on the quantity $\langle n \rangle$ is presented. One can see that the reliable location of objects for $\langle n \rangle < 4$ requires the considerable energy expenditure due to a great number of failures in the measurements of time intervals, and the obtained estimates will have a large dispersion.

Note that an increase in the slope of the leading edge of the pulse does not reduce considerably $\sigma^2(\langle n \rangle)$: due to the causality principle, the first event of the signal photoelectron formation always occurs after the instant of observation of the radiation pulse front, so that the estimate $\tilde{t}_{\mathrm{r}}^{\mathrm{th1}}$ proves to be positively shifted when the duration of the one-electron pulse tends to zero. For the same reason, the dispersions of the estimates $t_{\mathrm{r}}^{\mathrm{th1}}$ prove to be smaller than those of $\tilde{t}_{\mathrm{r}}^{\mathrm{th1}}$ for $\langle n \rangle > 40$ (Fig. 3a). The negative shift of the estimates $t_{\mathrm{r}}^{\mathrm{th1}}$ and $\tilde{t}_{\mathrm{r}}^{\mathrm{th1}}$ (Fig. 3b) is explained by the nonzero duration of the one-electron pulse. Analysis showed that the difference of $p_{\chi}(A)$ from the delta function leads to the increase in $\sigma^2(\langle n \rangle)$ by 3 % – 5 %.

Figure 4 shows the calculated dispersions $\sigma^2(\tau_{0.5})$ of estimates $t_{\mathrm{r}}^{\mathrm{g}}$ obtained for different values of $\langle n \rangle$ and T_{d}. One can see that the precision measurements of distances R to Earth satellites, whose confidence intervals can be estimated, taking into account the double propagation of radiation along the sighting line of the object, as

$$\Delta R = \pm 3\sigma(\langle n \rangle)c/2,$$

where c is the speed of light in the medium, are possible at rather long durations of probe pulses if the known condition $T_{\mathrm{d}} < 0.5\tau_{0.5}$ is fulfilled [9].

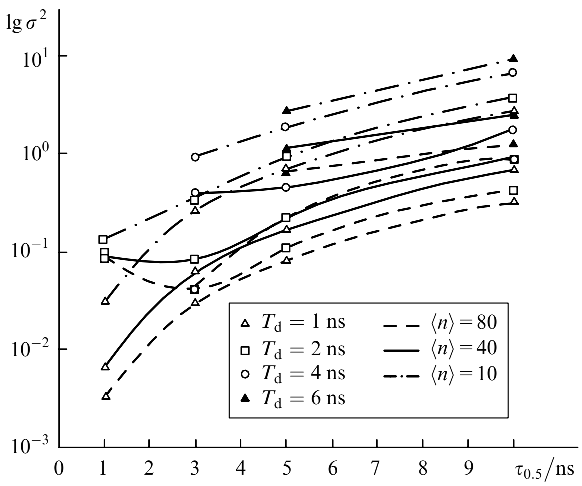

Figure 4. Dependences of the dispersions of estimates $t_{\mathrm{r}}^{\mathrm{g}}$ of the time position of the detected Gaussian pulse on the pulse duration $\tau_{0.5}$ for different digitising periods T_{d} and $\langle n \rangle$.

Of great interest are precision estimates of the distance R to the Earth satellites without a cube-corner reflector. In this case, the intensity of radiation scattered by the object surface is a function of time, the azimuth angle α, and the elevation angle β determining the orientation of the Earth satellite with respect to the laser ranging system, while the calculated value of $\hat{R}$ can substantially differ from the real distance R to the geometrical centre of the Earth satellite. The introduction of the correction function $\Psi(\hat{\alpha}, \hat{\beta})$, where $\hat{\alpha}$ and $\hat{\beta}$ are the estimates of the azimuth and elevation angles, which are obtained by recognising the observed aspect angle of the satellite from the envelope shape of $i(t)$ [10], noticeably reduces the measurement error of $\hat{R}$. By using the method of simulation of the current pulse envelope at the output of a photomultiplier described above, we can determine the probability characteristics of the recognition of the aspect angle of Earth satellites and estimate the measurement errors of R.

5. Conclusions

The results obtained in the paper show that the distance measurement error as small as 0.05 – 0.1 m can be achieved in one cycle of location of a remote object by detecting the counts of realisations of the current pulse envelope at the output of a photomultiplier and determining the position of the centre of gravity of this pulse at the time scale. Note that the above reasoning can be also applied to a great extent to cooled semiconductor PDs.

References

1. Perina J. *Quantum Statistics of Linear and Nonlinear Optical Phenomena* (Dordrecht: D. Reidel, 1984; Mir: Moscow, 1987).
2. Glauber R.J., in *Quantum Optics and Electronics* (New York: Gordon and Breach, 1965) p. 63; Moscow: Mir, Moscow, 1966) p. 91.
3. Mandel L. *Proc. Phys. Soc.*, **72**, 1037 (1958).
4. Berkovskii A.G., Gavanin V.A., Zaidel I.N. *Vakuumnye fotoelektronnye pribory* (Vacuum Photoelectronic Devices) (Moscow: Radio i Svyaz', 1988).
5. Vetokhin S.S., Gulakov I.P., Pertsev A.N., et al. *Odnoelektronnye fotopriemniki* (One-electron Photodetectors) (Moscow: Energoatomizdat, 1986).
6. Ivchenko G.I., Kashtanov V.A., Kovalenko I.N. *Teoriya massovogo obsluzhivaniya* (Queueing Theory) (Moscow: Vysshaya Shkola, 1982).
7. Lambert S.G., Casey W.L. *Laser Communications in Space* (Boston, London: Artech House, 1995).
8. Meleshko E.A. *Nanosekundnaya elektronika v eksperimental'noi fizike* (Nanosecond Electronics in Experimental Physics) (Moscow: Energoatomizdat, 1987).
9. Kulikov E.I., Trifonov A.P. *Otsenka parametrov signalov na fone pomekh* (Estimate of the Parameters of Signals Against the Noise Background) (Moscow: Sov. Radio, 1978).
10. Buryi E.V. *Kvantovaya Elektron.*, **25**, 471 (1998) [*Quantum Electron.*, **28**, 458 (1998)].